Yang S, Baker N, Mecrow BC, Hilton C,
Sooriyakumar G, Kostic-Perovic D, Fraser A.

Cost Reduction of a Permanent Magnet In Wheel Electric Vehicle Traction Motor.

In: International Conference on Electrical Machines (ICEM 2014).
2-5 September 2014, Berlin: IEEE.

DOI link to paper:

http://dx.doi.org/10.1109/ICELMACH.2014.6960218

Date deposited:

01/10/2014

Cost Reduction of a Permanent Magnet In-wheel Electric Vehicle Traction Motor

Sichao Yang[1], Nick J. Baker [1], B. C. Mecrow[1], Chris Hilton[2], Gunaratnam Sooriyakumar[2], D. Kostic-Perovic[2] and Al Fraser[2]

[1]School of Electrical, Electronic and Engineering, Newcastle University, Newcastle, United Kingdom

[2]Protean Electric Limited, Farnham, Surrey, United Kingdom

***Abstract* -- This paper describes a motor for use within the wheel of an electric vehicle. It demonstrates the influence of various rotor parameters on an outer rotor permanent magnet motor (ORPM) with Surface-mounted magnets (SM). The aim of this paper is to reduce the magnet volume, while maintaining the torque performance through the complete operating range. Six different magnet topologies are investigated firstly. Then, Semi Surface-mounted Permanent Magnet (SSPM), I shape tangential PM (IPM) and V shape interior PM (VPM) designs are compared in terms of torque capability at certain magnet volume. The VPM gives highest torque performance. The iron shielding concept in VPM can protect the magnets from the opposing armature flux, thus providing increased resistance to demagnetisation, and hence permitting thinner magnets. Furthermore, a new slot/pole combination with higher torque capability has been studied. However, due to the increased inductance, motor with V shape design needs to work at a poorer power factor and consequently a reduced speed range for a given inverter. Lastly, Cost effective and simple manufacture method of the VPM rotor is also addressed with consideration of mechanical feasibility.**

***Keywords* – Cost Reduction, In-wheel Motor, Outer Rotor, V shape magnets**

I. INTRODUCTION

In recent decades, attention on Electric Vehicles (EVs) has been greatly increased due to their high efficiency, lack of emissions and reduced noise pollution. However, high initial cost and a short driving range are two major problems for the electric propulsion system. The required high power and torque density leads the designer to use Permanent Magnet Machines, which along with the power electronic inverter and the batteries, produce a high initial cost.

The cost ratio between motor materials is given as PM : Cu : Si-Steel = 10 : 1 : 0.15 in [1].

Therefore, there is a drive to reduce the magnet content, whilst keeping the motor cost effective, efficient and compact. The motors in question, manufactured by Protean Electric, are mounted in the wheel of the vehicle ensuring that all the motor output torque is available at the wheel, giving the customer better control and improving efficiency and compatibility by eliminating parts of mechanical design, such as gears and differentials, at the cost of increased size and weight of the motor. In this project, the motor used as the benchmarking motor is a high-torque, low-speed, outer rotor permanent magnet motor with a good overload capability, wide speed control range, and designed to fit within a 16" wheel-rim. Basic performance parameters are shown in Table I.

The aim of this project is to reduce the cost of the motor by: 1.) using less magnet material; 2.) lowering the magnet grade; 3.) simplifying assembly and manufacturing methods; 4.) recycling scrap more efficiently. The reduction of magnet volume is the sole focus in this paper.

II. BENCHMARKING MOTOR

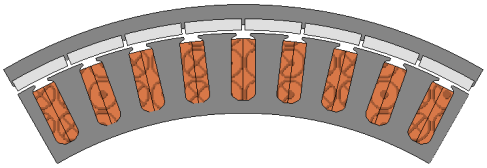

Fig. 1. 2D model for one sub motor of the benchmark machine

Fig. 1 shows a 2D model of 1/6 of the existing outer rotor permanent magnet motor. This machine is here referred to as the benchmarking motor (BMM). The motor has a concentrated double-layer winding, with each coil wound round a single tooth, as illustrated in Fig. 2. The primary motor parameters are listed in Table I:

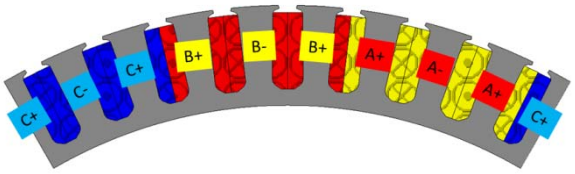

Fig. 2. Winding configuration for three phases of the motor

Rated DC supply Voltage	240	V
Rated Phase Current (peak & sine)	60	A
Rated Output Torque	350.22	Nm
Base Speed	482	rpm
Rated Output Power	17.7	kw
Maximum speed	1000.0	rpm
Overloading DC Voltage	400	V
Overloading Phase Current (peak & sine)	90	A
Control Strategy	SVPWM	
Coolling Method	Water Jacket	
Magnet	NdFeB-N45SH	
Magnet Thickness	4	mm
Magnet Temperature	100	deg
Overall motor axial length	35	mm
Outer Diameter	340	mm
Inner Diameter	264	rpm
Air Gap	1	mm
Rotor Thickness	9	mm
Slot Number	54	-
Pole Number	48	-

Table I Benchmarking Motor Parameters

The BMM design was driven by standard wheel dimensions and required torque performance. The axial length is constrained to 35mm, and so concentrated winding configuration is selected to ensure a non-overlapping end-winding. As a given air-gap force produces a torque

proportional to its radius, to maximize torque, the largest possible air-gap radius is chosen. The outer diameter is constrained by the wheel size, so the air-gap radius is maximized by increasing the number of pole pairs to reduce the required rotor core back depth. 48 poles were found to be a good compromise. The motor is low speed direct-driven, and the electric frequency at maximum speed (1000rpm) is 400Hz; iron loss in the motor is manageable and the frequency of switching of the inverter does not create undue switching loss.

A fractional number of slots per pole used as a smaller number of slots for a given number of poles gives a distinct manufacturing advantage and is also conducive to low cogging torque. It also enables a significant increase in the achievable machine inductance to facilitate constant power operation over a wide speed range with flux weakening control, explained in detail in [3] and [4].

For fault tolerance, the machine can be split into two, three or six independent sub-motors. Multiphase designs in [5, 6, 7] decouple the flux from each phase with fault-tolerant teeth. In this machine, multiphase sub-motors are adopted. This arrangement offers sufficient fault tolerant capability when sub motors fail. A general description of the machine and testing of the thermal, mechanical and electromagnetic independence of each sub is conducted in [8].

In order to be cost-competitive in the automobile market, the volume of magnet, which is the most expensive material in the motor, needs to be reduced. Therefore, alternative rotor topologies are studied to seek better magnet utilization and compared to this benchmarking motor

III. ROTOR TOPOLOGIES

In the analysis of the benchmarking motor, one important conclusion is made by observing the impact of magnet thickness on the magnet utilization: in essence this is the torque capability per unit magnet mass. As the magnet thickness is reduced, which can be seen in Fig. 4, the magnet utilization can be improved rapidly due to the improved overall permeability in a less saturated magnetic flux flowing circuit as indicated from Fig. 3 - also stated in [9].

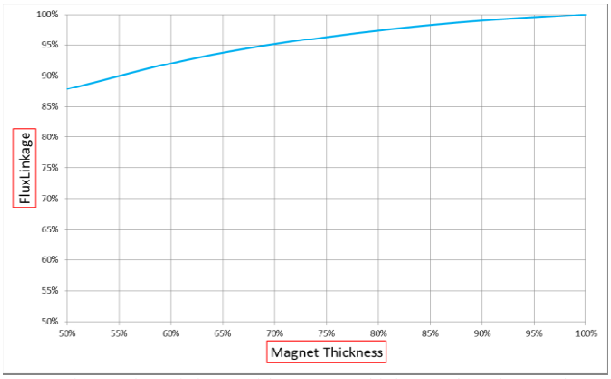

Fig. 3. Flux Linkage with Magnet Thickness changing on the benchmarking motor

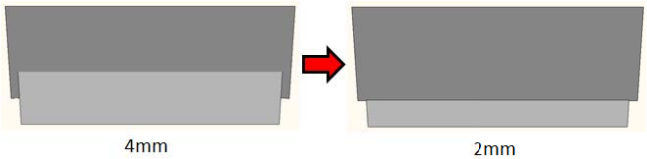

Fig. 4. The Magnet Thickness change in the benchmarking motor

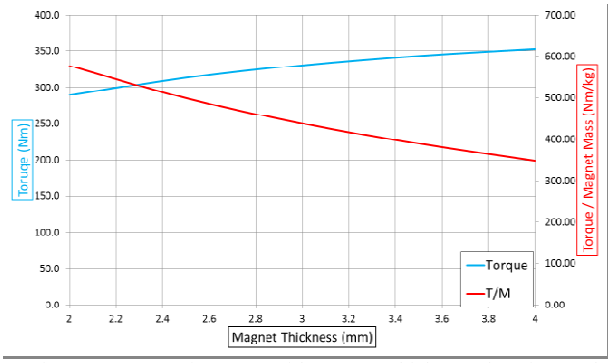

Fig. 5. Torque Performance with Magnet Thickness changing on the benchmarking motor

By halving the magnet thickness to 2mm, as shown in Fig. 4, the value of Torque / Magnet Mass, which is illustrated with the red curve in Fig. 5, is improved by 65% whilst the peak torque at rated load is only reduced by 18%.

The electric loading must be high due to the high torque density demand. The stator is covered with a fluid cooling jacket, but it is still relatively difficult to remove rotor losses near the air gap periphery. The temperature of the magnets is expected to be 100 degrees under continuous running. Hence, demagnetisation is a potential issue when reducing the magnet volume, as can be seen from Fig. 6. *The blue regions indicate the flux density is above the magnet knee-point and the red regions indicate where demagnetisation is occurring.*

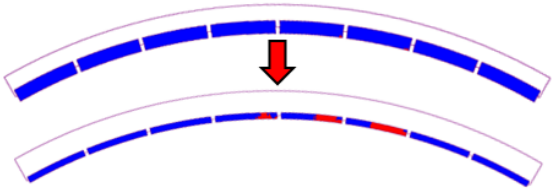

Fig. 6. Demagnetization analysis in the benchmarking motor under overload conditions

The benchmarking motor is not demagnetized with 90Amps peak over-loading current input, but as soon as the magnets are narrowed demagnetisation occurs. So the new magnet topologies are now investigated to seek possible solutions.

In general there are three categories of permanent magnet rotor: surface-mounted magnet, surface-inserted magnet and interior magnet. According to [10], the interior magnet rotor has better demagnetisation resistance. Six new models with different magnet positions were modelled and compared in terms of peak torque performance and demagnetisation resistance at the rated condition, as shown in Fig. 7:

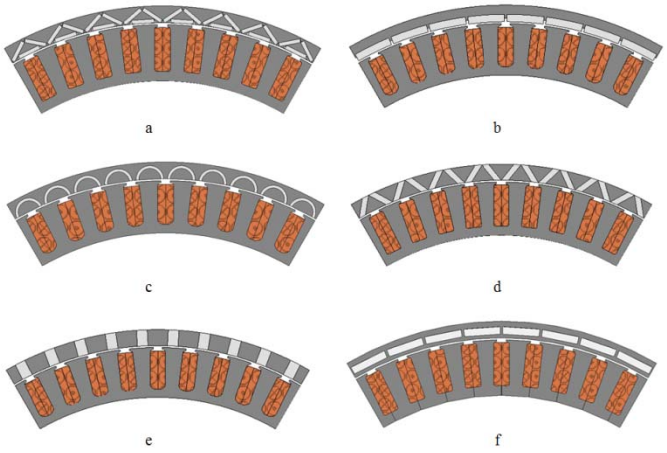

Fig. 7. Cross sections of: a.) Triangle PM; b.) Surface-mounted PM; c.) C-shaped PM; d.) V-shaped PM; e.) Spoke type PM; f.) Buried PM

In this study the Stator design is unaltered and the total rotor depth is fixed at 9 mm, which only leaves 5 mm core back in the Surface-mounted Permanent Magnet (SMPM). The flux is highly saturated in the Buried Permanent Magnet (BPM) design and torque performance is consequently poorer. The Triangle shape is developed based on the motor shown in [11]. After its primary optimisation, the peak torque value is similar to the benchmarking motor, but using less magnet material. The idea of a C shape design, which is expressed in [12], is similar to the V shape: it produces flux concentration and increased inductance. Consequently, the C shape, V shape and spoke shape designs give a higher torque density in comparison with the benchmarking motor. However, V shape PM and spoke shape PMs were selected for further study due to their relatively simple manufacturing process.

IV. V SHAPE DESIGN

In Fig. 8, the best performance is seen in the V shape design. The blue line stands for the benchmarking motor, whose upper bound of magnet mass is its original value. Correspondingly, the magnet mass is reduced to half by thinning the magnets at its lower bound. Similarly, the magnet volume is reduced by changing the thickness in the V and Spoke designs as shown in Fig. 9 and Fig. 10.

The V shape can give the same torque with 56% of the magnet mass, whilst the spoke shape needs to use 78% of the original material to generate the same torque.

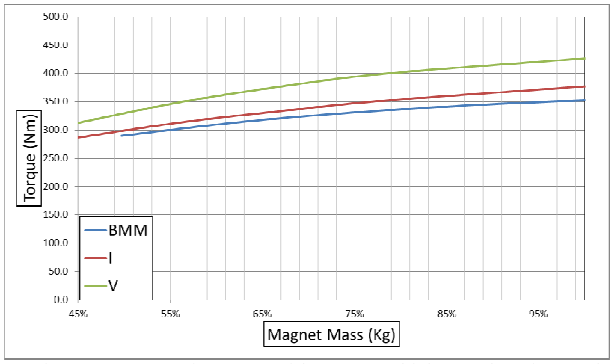

Fig. 8. Torque Performance with Magnet Thickness changing on the benchmarking motor, V shape PM and Spoke shape PM

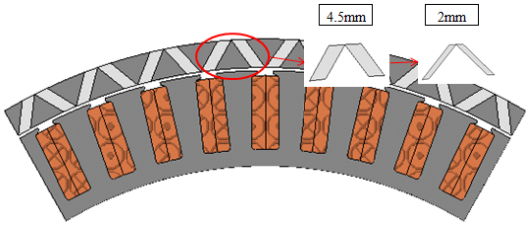

Fig. 9. The Magnet Thickness change in V shape PM

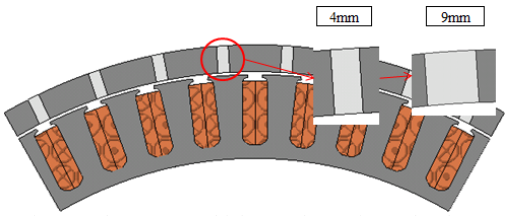

Fig. 10. The Magnet Thickness change in Spoke shape PM

As for the demagnetization issue: the V shape design has no demagnetisation under the same over-loading condition, as shown in Fig. 11. This is because the iron piece in front of the magnets acts as a protecting shield, protecting the magnet from high armature magnetising field strength at the slot opening, as seen in Fig. 12.

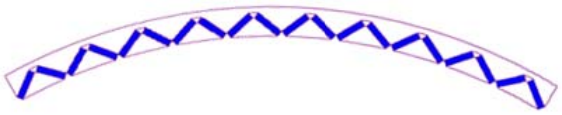

Fig. 11. Demagnetization analysis in VPM

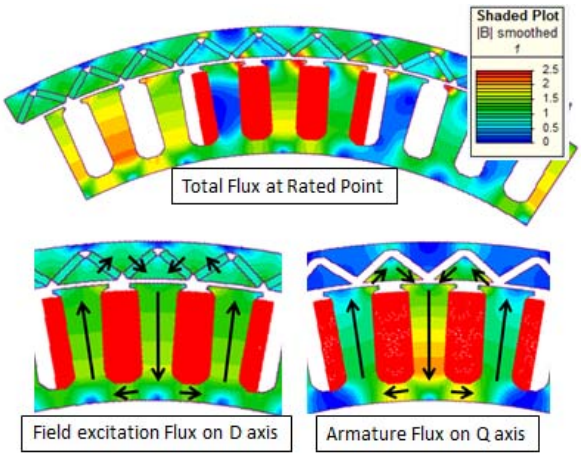

Fig. 12. Field plot with Flux flowing direction in V shape design

The variation of spoke shape has been studied and no performance improvement has been found. Therefore, further development is focused on the V shape design.

Fig. 13 and Fig. 14 show the torque capability of the original, surface mounted, benchmarking design, and the V shaped design at rated condition. The separate torque curves on full current advance angle range are generated by frozen permeability method.

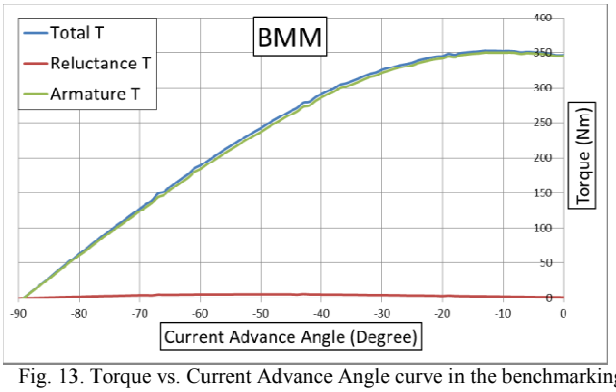

Fig. 13. Torque vs. Current Advance Angle curve in the benchmarking motor

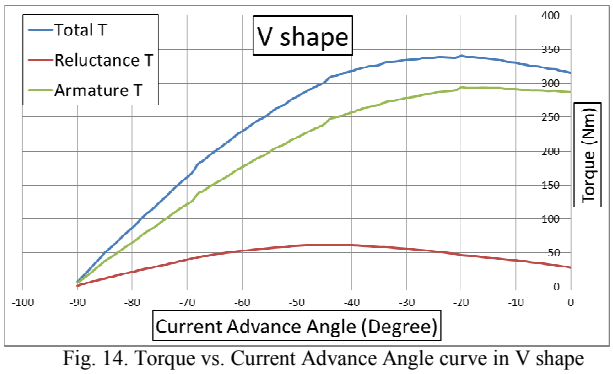

Fig. 14. Torque vs. Current Advance Angle curve in V shape

Due to the contribution of the reluctance torque in the V shape design, the magnet volume can be reduced significantly whilst maintaining the torque output. The comparison of peak torque values in different designs is given in Fig. 15. The benchmarking motor with 56% of the magnet volume gives the lowest torque output, whereas the V shaped design with 56% magnet volume has 97% peak torque compared to the benchmarking motor.

Therefore, the V shaped design with matched torque performance compared to BMM is chosen to be modified in concern of mass production.

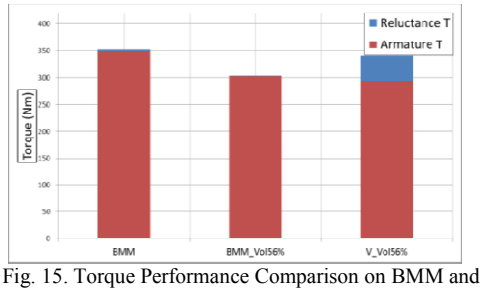

Fig. 15. Torque Performance Comparison on BMM and V

V. V SHAPE MODIFICATION

A. *Pole / Slot number investigation*

The level of flux concentration within the V shaped design is a function of the magnet width compared to the air-gap arc over which it spans. For a fixed rotor radial depth, this ratio reduces with increasing pole number. In order to understand the impact on performance for a given magnet, different pole numbers have been investigated. As before, the stator design remains unchanged with 54 slots. By increasing the pole number from 48 to 60 and retaining the same magnet thickness and its overall mass, the design changes as shown in Fig. 16. The 60 pole design has a higher torque capability for a given stator current.

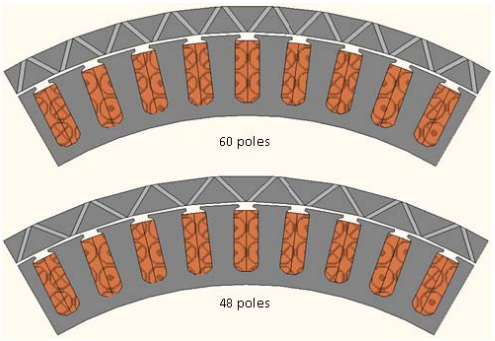

Fig. 16. Rotor Topology in two V shape Designs

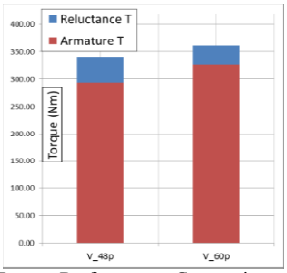

Fig. 1 Torque Performance Comparison on V design

Compared to the BMM, torque capability is maintained in the new design. However, the increased electrical frequency demanding at the same mechanical speed results in increased d and q axis inductance. In turn, this results in a lower base speed for the machine. This situation is particularly severe in the higher pole number design. The torque against speed envelope is illustrated in Fig. 17:

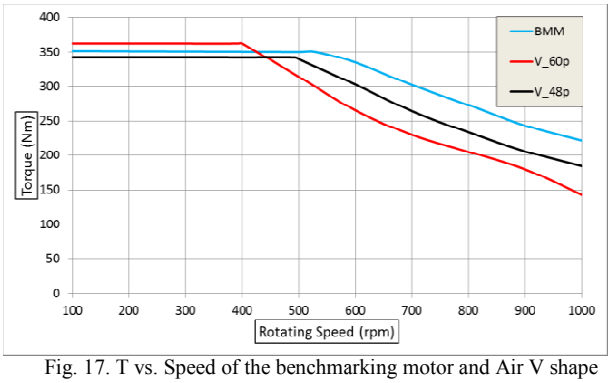

Fig. 17. T vs. Speed of the benchmarking motor and Air V shape

The base speed of the V shape design with 60 poles is 343rpm, compared to 482rpm in the benchmarking motor with 48 poles, which means the 6% higher torque capability is obtained with the cost of losing 25% of its rated output power. This could only be overcome by increasing the VA rating of the inverter.

However, when the same test is performed on the V shape design with 48 poles, the base speed is extended to 452rpm. The VA rating can thus be retrieved at the cost of slightly less torque in comparison to the higher pole number design.

Then, the number of coil turns is changed in both V48 poles design and V60 poles design to match with the rated torque in BMM. With the same rated current value, the base

speed of BMM, V48p and V60p are 529rpm, 469rpm and 415rpm, respectively.

The 48 poles design is remained due to higher output power compared to the 60 poles design.

B. *Loss analysis*

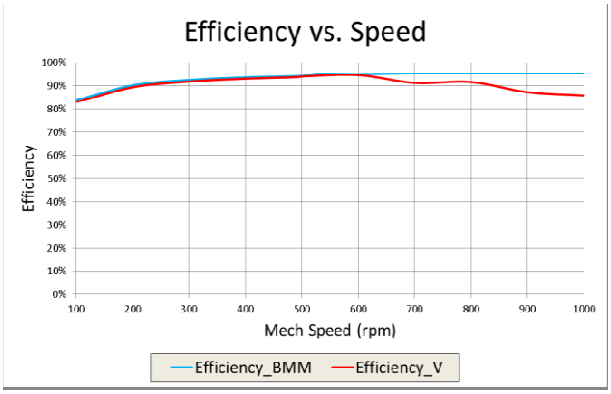

Fig. 2 efficiency on full speed range

As can be seen from Fig. 2, the efficiency drops while speed is increasing above base speed point. This is due to the relatively higher current advance angle for field weakening control in V shape and its high content of harmonics.

The study to reduce the loss at high speed and to reduce the material cost by replacing the back lamination with solid iron stack is still under study at the time of writing this paper.

C. *Manufacturing consideration*

In order to ease the manufacturing process and increase the assembly speed, it is preferred mechanically for the rotor lamination to be a single piece, as shown in Fig. 18:

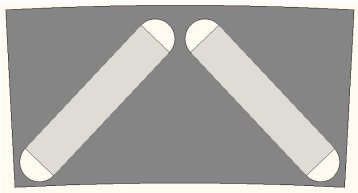

Fig. 18. Conventional V shape

However, this arrangement creates two flux leakage paths at either end of the magnet, which reduce the torque by 20%.

Several designs have been created and analysed to block the flux leakage path, as shown in Fig. 19:

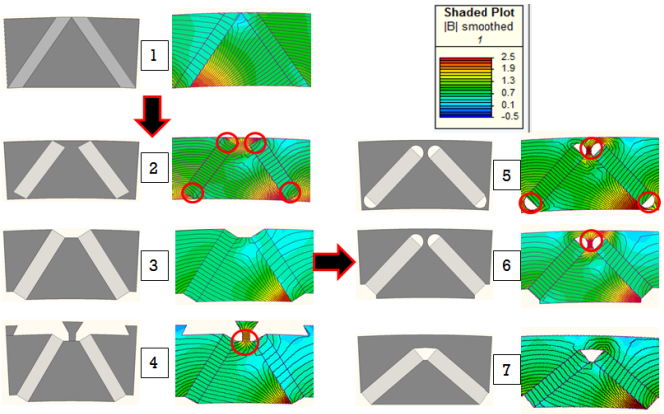

Fig. 19. V shape modifications

The ideal V shape design is design 1. The magnets are made rectangular in design 2 to reduce material waste and ease the magnet cutting process. However, the red circles indicate the flux leakage paths, which are eliminated in design 3. Now the single piece lamination is made into multi-pieces, which is difficult to assemble onto the rim. The key shaped mechanical feature is introduced in design 4 to support the inner rotor piece, hold outer rotor pieces together and locate the rotor pieces. However, the key results in additional leakage flux, which reduces the flux linkage.

Hence, the conventional design 5 is improved by cutting off the inner flux flowing path in design 6, while keeping the rotor back lamination in one piece.

In design 7, the outer flux flowing path is blocked by introducing an air bridge, which reduces flux leakage on the outer joint of the magnets. Also, there is no leakage path on the inner joint of the two magnets because of lack of iron in that area. Moreover, there is only one point on each magnet sitting on the periphery of the inner rotor radius, which means the demagnetization resistance is further increased by preventing the magnet from directly opposing the armature flux travelled across the air-gap.

The field view is shown in Fig. 20 and the torque performance in these designs is shown in Fig. 21 . The torque performance of design 7 gives the closest result to design 1 (the ideal design) whilst making manufacture and assembly simple due to a single core back lamination.

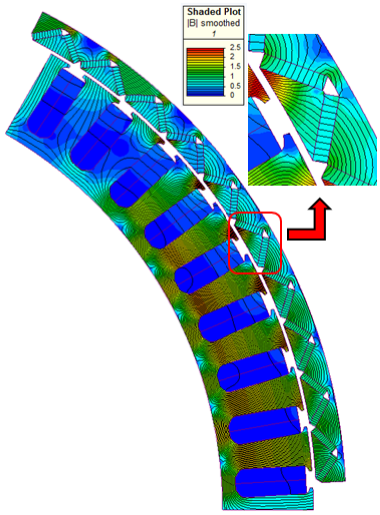

Fig. 20. The field view of Air Bridge V

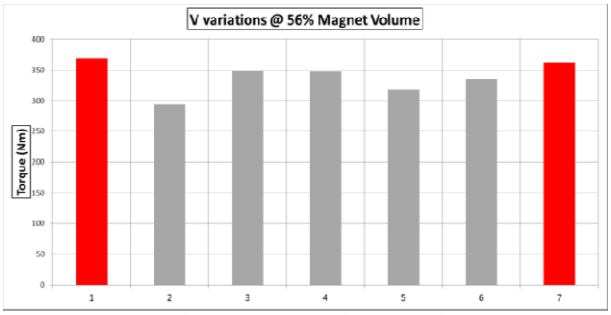

Fig. 21. Torque Performance Chart

In summary, the peak torque value of the V shape design has deteriorated by using a conventional way to gain an easy

manufacturing process. Therefore, a new air-bridge design is created in the V shape which maintains its peak torque performance with a single outer rotor piece. This new design shape includes an air bridge on two adjacent magnets which form one pole.

D. Mechanical feasibility

In the rotor there are two forces on the rotor pieces, namely the centrifugal force due to the rotation and the magnetic attractive force from the adjacent magnets and the facing teeth across the air gap. The centrifugal force is not considered a problem in this application, as the outer rim can hold the rotor together. The magnetic force has been simulated in MagNet by winding one coil around the closest tooth facing the testing rotor piece and injecting the maximum current, as it is shown in Fig. 3.

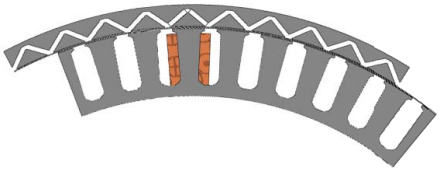

Fig. 3 The magnet attractive force test on the inner rotor piece

The worst scenario for force is illustrated in Fig. 4, where the peak value of the overload phase current (90A) has the opposite polarity of the magnets, which attracts the triangle piece, at a standstill. Together with Fig. 5, both the direction and the value of the forces are presented in Table 2. To withstand this amount of force, the rotor pieces and magnets would be glued onto the rotor back.

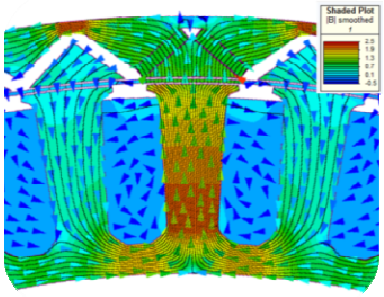

Fig. 4 The field view of the flux travel path

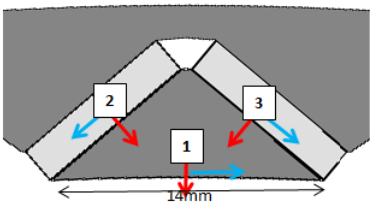

Fig. 5 the direction of the force on each piece

	number	1	2	3	
force	perpendicular	67.37	2.01	1.93	Nm
	tangential	1.79	-22.17	-19.68	

Table 2 the exerted force on each piece ('–' sign means the direction of the force is opposite to the reference direction)

With further optimisation process, it was found that the rotor core back depth could be reduced, resulting in 7% further reduction in magnet volume, but only 4% reduction in torque capability. This is shown in Fig. 22. The simulation results are shown in Table III:

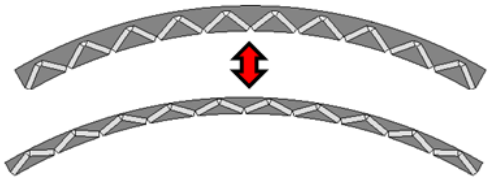

Fig. 22. Rotor Outer Radius change: 170mm to 166.5mm

V-air

Torque	R_OR	Mass
Nm	mm	Kg
361.34	170	0.094
347.50	166.5	0.088

BMM

Torque	R_OR	Mass
Nm	mm	Kg
352.00	170	0.168

Table III Parameters of Air V and benchmarking motor

Thus, the manufacturing cost is further reduced with less steel volume. Meanwhile, other potential aspects like lower material grade and changing rotor diameter to stator diameter split ratio are under study.

VI. CONCLUSION

With careful choice, it is possible to greatly decrease the magnet volume employed in surface mounted magnet rotors, without major loss of performance or increased risk of demagnetization. A surface mounted magnet benchmarking motor is replaced with V shape magnets, saving 44% of the magnet mass. The demagnetization resistance is improved and detailed modifications are made to accommodate mass production. The V shape design results in an increase in inductance, which must be closely monitored. If the inductance becomes too large then there is a significant reduction in the torque – speed envelope of the machine.

VII. ACKNOWLEDGMENT

The authors acknowledge the contributions of Chukwuma J. Ifedi for his work on the previous version of this Application.

VIII. REFERENCES

[1] C. Cheol Min, S. Jung Hoon, and N. Kwang-Hee, "Comparative study of EV propulsion motors for A-class vehicles," in *Electrical Machines and Systems (ICEMS), 2011 International Conference on*, 2011, pp. 1-3.

[2] T. Finken, M. Hombitzer, and K. Hameyer, "Study and comparison of several permanent-magnet excited rotor types regarding their applicability in electric vehicles," in *Emobility - Electrical Power Train, 2010*, 2010, pp. 1-7.

[3] D. Evans, Z. Azar, L. J. Wu, and Z. Q. Zhu, "Comparison of optimal design and performance of PM machines having non-overlapping windings and different rotor topologies," in *Power Electronics, Machines and Drives (PEMD 2010), 5th IET International Conference on*, 2010, pp. 1-7.

[4] W. Jiabin, K. Atallah, Z. Q. Zhu, and D. Howe, "Modular Three-Phase Permanent-Magnet Brushless Machines for In-Wheel Applications," *Vehicular Technology, IEEE Transactions on,* vol. 57, pp. 2714-2720, 2008.

[5] Q. Chen, G. Liu, L. Sun, Y. Jiang, and J. Yang, "Comparison of five topologies rotor permanent magnet motors with improved fault-tolerance," in *Industrial Electronics (ISIE), 2013 IEEE International Symposium on*, 2013, pp. 1-5.

[6] C. Qian, L. Guohai, Y. Junqin, G. Wensheng, and Z. Wenxiang, "Comparison Of Two Interior Permanent-Magnet Motors With Improved Fault-Tolerance," in *IECON 2012 - 38th Annual Conference on IEEE Industrial Electronics Society*, 2012, pp. 4093-4098.

[7] L. Guohai, G. Wensheng, C. Qian, J. Linni, S. Yue, and Z. Wenxiang, "Design and analysis of new fault-tolerant permanent magnet motors for four-wheel-driving electric vehicles," *Journal of Applied Physics,* vol. 111, pp. 07E713-07E713-3, 2012.

[8] C. J. Ifedi, B. C. Mecrow, S. T. M. Brockway, G. S. Boast, G. J. Atkinson, and D. Kostic-Perovic, "Fault-Tolerant In-Wheel Motor Topologies for High-Performance Electric Vehicles," *Industry Applications, IEEE Transactions on,* vol. 49, pp. 1249-1257, 2013.

[9] K. Mi-Jung, C. Su-Yeon, L. Ki-Doek, L. Jae-Jun, H. Jung-Ho, J. Tae-Chul*, et al.*, "Torque Density Elevation in Concentrated Winding Interior PM Synchronous Motor With Minimized Magnet Volume," *Magnetics, IEEE Transactions on,* vol. 49, pp. 3334-3337, 2013.

[10] K. Ki-Chan, K. Kwangsoo, K. Hee-Jun, and L. Ju, "Demagnetization Analysis of Permanent Magnets According to Rotor Types of Interior Permanent Magnet Synchronous Motor," *Magnetics, IEEE Transactions on,* vol. 45, pp. 2799-2802, 2009.

[11] K. Yamazaki, M. Kumagai, T. Ikemi, and S. Ohki, "A Novel Rotor Design of Interior Permanent Magnet Synchronous Motors to Cope with Both Maximum Torque and Iron Loss Reduction," *Industry Applications, IEEE Transactions on,* vol. PP, pp. 1-1, 2013.

[12] K.-j. Lee, K. Kim, S. Kim, J.-S. Ahn, S. Lim, and L. Ju, "Optimal magnet shape to improve torque characteristics of interior permanent magnet synchronous motor," *Journal of Applied Physics,* vol. 97, pp. 10Q505-10Q505-3, 2005.

IX. BIOGRAPHIES

Sichao Yang received a BE degree in Electric and its Automation Control from South West University for Nationalities, China, in 2011, and a MSc degree in Electrical Power from Newcastle University, UK, in 2012. He is currently working towards the PhD degree in Newcastle University, designing a high torque, fault tolerant and cost competitive In-wheel motor for Electric Vehicles, which is sponsored by Protean Electric.

Nick J. Baker received a MEng Degree in Mechanical Engineering from Birmingham University, UK, in 1999 and a PhD from Durham University, UK, in 2003 for work in electrical machine design for marine renewable energy devices. He subsequently worked as an academic at Lancaster University (2005-2008), a renewable energy consultant at TNEI and presently a Lecturer at Newcastle University's Power Electronics Machines and Drives Group. Nick is a machine designer with research projects across the automotive, aerospace and renewable energy sector.

Barrie C. Mecrow is Professor of Electrical Power Engineering and head of the School of Electrical and Electronic Engineering at Newcastle University, UK. His research interests include fault tolerant drives, high performance PM machines and novel switched reluctance drives. He is actively involved with industry in the aerospace, automotive and consumer product sectors, who fund a large range of projects. Barrie commenced his career as a turbo-generator design engineer with NEI Parsons, England. He became a lecturer at the University of Newcastle in 1987 and a professor in 1998.

Chris Hilton is the Chief Technology Officer at Protean Electric with particular responsibility for advanced research, systems design, systems engineering and intellectual property. He has previously held roles in the fields of communications electronics, satellite navigation and particle physics research. Chris holds a PhD in physics from the University of Manchester, UK, and a first class honours degree in mathematics from the University of Cambridge, UK.

Gunaratnam Sooriyakumar is a Senior Development Engineer at Protean Electric Limited, UK where he is working on development of electric motor drives for automotive application. He obtained BSc in Electrical and Electronic Engineering from University of Peradeniya, Sri Lanka. He obtained his PhD from UEL with the sponsorship from Emerson industrial automation. He worked for Emerson industrial automation where he was the leader for R&D team which has developed the commercially successful next generation electric motors with higher torque density and high dynamic capability for industrial automation application. In addition he provided his expertise to improve the bespoke products at Emerson industrial automation which includes various kinds of electric motors for military and aerospace application. After leaving Emerson Industrial Automation, he continued working as an engineering consultant for Emerson industrial automation at Andover and for a wind generator design company at Edinburgh until joining Protean Electric Limited.

Dragica Kostic Perovic gained her first degree in electrical engineering at the University of Belgrade, Serbia, and her DPhil at the University of Sussex, UK. She is a Principal Motor Design Engineer at Protean Electric with main interests in the area of electromagnetic motor design, and DFMEA as a design process.

Alexander Fraser worked as a Senior Mechanical Systems Engineer at Protean Electric with a focus on motor conceptual design and dealing with vehicle-level engineering solutions related to the integration of in-wheel motors onto vehicle platforms. He holds a BEng Honours Degree in Automotive Engineering from Oxford Brookes University, UK.